Polygenic pathways shape white matter vulnerability to Alzheimer's disease-related pathophysiological changes

Tranfa, Mario; Pieperhoff, Leonard; Pontillo, Giuseppe; Luckett, Emma S.; Collij, Lyduine E.; Oliveira, Tiago Gil; Tesi, Niccoló; Vilor-Tejedor, Natalia; Reinders, M.J.T.; More Authors

DOI
10.1186/s13195-025-01888-3

Publication date
2025

Document Version
Final published version

Published in
Alzheimer's Research and Therapy

Citation (APA)
Tranfa, M., Pieperhoff, L., Pontillo, G., Luckett, E. S., Collij, L. E., Oliveira, T. G., Tesi, N., Vilor-Tejedor, N., Reinders, M. J. T., & More Authors (2025). Polygenic pathways shape white matter vulnerability to Alzheimer's disease-related pathophysiological changes. *Alzheimer's Research and Therapy*, *17*(1), Article 240. https://doi.org/10.1186/s13195-025-01888-3

Tranfa *et al. Alzheimer's Research & Therapy* (2025) 17:240
https://doi.org/10.1186/s13195-025-01888-3

Alzheimer's Research & Therapy

RESEARCH Open Access

Polygenic pathways shape white matter vulnerability to Alzheimer's disease-related pathophysiological changes

Mario Tranfa[1,2*], Leonard Pieperhoff[1,3], Giuseppe Pontillo[1,2,4,5], Emma S. Luckett[1,6,7], Lyduine E. Collij[1,3,8], Tiago Gil Oliveira[9,10,11], Niccoló Tesi[12,13], Natalia Vilor-Tejedor[14,15,16,17], André Altmann[18], Luca Roccatagliata[19,20], Matteo Pardini[19,21], Henne Holstege[12,22,23], Marcel Reinders[13], Pierre Payoux[24,25], Pablo Martinez-Lage[26], Craig W. Ritchie[27,28], Adam Waldman[29,30], Joanna M. Wardlaw[29,31], Juan Domingo Gispert[14,15,32,33], Gemma Salvadó[8], Arturo Brunetti[2], Henk J.M.M. Mutsaerts[1,3], Alle Meije Wink[1,3], Frederik Barkhof[1,4,18,34] and Luigi Lorenzini[1,3,21]

Abstract

Background The accumulation of amyloid-β_{1-42} ($A\beta_{1-42}$) peptides and phosphorylated-Tau_{181} (p-Tau_{181}) tangles from the preclinical stages of Alzheimer's disease (AD) has led to a biological definition of the disease. However, among $A\beta_{1-42}$-positive individuals, cognitive decline onset varies, and some never develop symptoms. Genetic influences on molecular pathways and their interactions with proteinopathy may underlie this heterogeneity. Leveraging data from a large sample of cognitively intact older adults in the European Prevention of Alzheimer Dementia (EPAD) cohort, we examined how AD-related pathophysiological changes (i.e., $A\beta_{1-42}$ and p-Tau_{181}), polygenic pathways and their interaction are associated with WM micro- and macrostructural properties.

Methods We selected 803 individuals (mean age = 64.7 ± 7.3 years, 458 [57.0%] females, 275 [34.2%] *APOE*-ε4 carriers) with CSF-$A\beta_{1-42}$ and p-Tau_{181} measurements available, full genotyping, and structural and diffusion MRI. Polygenic risk scores (PRSs) were computed using 85 AD-related genetic variants. These were mapped to their corresponding genes and, after excluding those belonging to the *APOE* locus, clustered by function into six pathway-specific PRSs (i.e., immune activation, signal transduction, inflammation, lipid, amyloid, and clearance pathways). Diffusion MRIs were processed through the fixel-based analysis framework to derive fiber density (FD) and fiber cross-section (FC) metrics, which were averaged within WM tracts. Linear models assessed the effects of AD-related pathophysiological changes, global and pathway-specific PRSs, and their interactions on FD and FC at both the tract and fixel levels. Models were corrected for multiple comparisons.

Results P-Tau_{181} was primarily associated with greater FD. The lipid pathway was associated with greater FD and FC, with these effects predominantly occurring in the left hemisphere, consistent with evidence of hemispheric dominance. The clearance pathway moderated the effect of $A\beta_{1-42}$ on FD, with a positive slope in A + compared

*Correspondence:
Mario Tranfa
m.tranfa@amsterdamumc.nl

Full list of author information is available at the end of the article

to A- individuals. The immune activation pathway moderated the effect of p-Tau$_{181}$ on FD, with a negative slope in T + compared to T- individuals.

Conclusions Pathway-specific genetic vulnerability to AD is associated with alterations in WM tracts both directly and by moderating the effects of AD-related pathophysiological changes. AD-associated genetic risk should be integrated into the AD diagnostic framework to enable targeted screening and intervention for future preclinical trials aimed at specific biological pathways.

Keywords Alzheimer's disease, Polygenic risk scores, Polygenic pathways, White matter, Fixel-based analysis, Diffusion magnetic resonance imaging

Background

The accumulation of amyloid-β$_{1-42}$ (Aβ$_{1-42}$) peptides and phosphorylated-Tau$_{181}$ (p-Tau$_{181}$) tangles is the neuropathological hallmark of Alzheimer's disease (AD), the leading cause of dementia worldwide [1]. Substantial evidence indicates that this process precedes the clinical onset by decades [2], thus intervention studies have increasingly focused on preclinical stages [3], leading to the adoption of a biological definition of AD [4]. However, among Aβ$_{1-42}$-positive individuals, the age at onset of cognitive deficits varies, and some may never develop AD symptoms [5], suggesting heterogeneous responses to neuropathological change [6]. Efforts to unravel this variability have underscored the predominant role of genetic heritability in AD, with genetic factors estimated to account for approximately 70% of disease risk based on twin studies [7]. Genome-wide association studies of AD have identified more than 80 genetic variants associated with a modification of the risk of developing the disease [8]. By combining these variants, it is possible to generate a genetic risk score of an individual, estimating their likelihood of developing AD-related dementia or escaping the disease [8]. Identified genes span diverse molecular pathways extending beyond the direct production of Aβ$_{1-42}$ and p-Tau$_{181}$, including immune cell and microglial activation, synaptic vulnerability and Aβ$_{1-42}$ clearance [9]. Based on their biological function, these genes can be clustered to compute pathway-specific polygenic risk scores (PRSs), offering insight into individual vulnerability [10]. Moreover, emerging evidence suggests that these genes and pathways act in a disease stage-dependent manner [11], raising critical questions about their interaction with the progressive accumulation of Aβ$_{1-42}$ and p-Tau$_{181}$. It is increasingly clear that the path to neurodegeneration and dementia is unique for each individual. Matching the right treatment to the appropriate population is essential for advancing precision medicine and optimizing clinical trials [12].

In this context, white matter (WM) disruption has emerged as a crucial pathological driver in the AD cascade. It has been postulated that Aβ$_{1-42}$ and p-Tau$_{181}$ deposition represent a homeostatic response to age-dependent myelin breakdown, potentially leading to neurodegeneration and dementia depending on individual genetic vulnerability [13, 14]. Moreover, WM actively facilitates the spread of p-Tau$_{181}$ between connected gray matter regions [15] and contributes to Aβ$_{1-42}$ deposition, as oligodendrocytes produce Aβ$_{1-42}$ alongside neurons [16]. Evidence also suggests that WM disruption precedes cortical atrophy in AD [17, 18], positioning WM alterations as promising early biomarkers of disease progression. However, conventional diffusion imaging techniques face limitations in disentangling the complex microstructural organization of WM. To overcome this, fixel-based analysis (FBA) of diffusion MRI has been developed, enabling the study of multiple WM populations within a voxel, referred to as fixels [19]. By providing quantitative metrics such as fiber density (FD) and fiber cross-section (FC), FBA offers a powerful tool for characterizing WM tracts micro- and macrostructural alterations in AD and their relevance to genetic heterogeneity. Previous studies have demonstrated the sensitivity of fixel metrics to AD-related WM disruption [20–23], showing variable alterations in FD and FC depending on the disease stage. Nevertheless, the relationship between these alterations and AD-related pathophysiological changes remains unclear. Some findings suggest that WM alterations may occur independently of Aβ$_{1-42}$ [21, 22], while others associate them with its accumulation [20, 23]. Conversely, p-Tau$_{181}$ appears to exert limited effects on WM [22, 23]. Overall, these findings suggest a multiphasic relationship and underscore the need to look beyond Aβ$_{1-42}$ and p-Tau$_{181}$ to fully understand the complex processes driving AD-related brain alterations. Clarifying the associations between molecular pathways, AD proteinopathy and WM fibers integrity in the early and preclinical stages of the AD continuum is increasingly important for developing effective screening strategies and tailored interventions in primary and secondary prevention trials [3].

Here, leveraging data from a large sample of non-demented older adults from the European Prevention of Alzheimer Dementia (EPAD) cohort [24], we aimed to assess (i) the association of AD-related pathophysiological changes (i.e., Aβ$_{1-42}$ and p-Tau$_{181}$) and (ii) pathway-specific AD PRSs, (iii) as well as their interaction, with

WM micro- and macrostructural integrity using the FBA framework.

Methods

The study workflow is depicted in Fig. 1. The study was approved by the ethical committees of all participating centers. All study participants provided written informed consent according to the Declaration of Helsinki.

Participants

Data were drawn from the latest data release from the European Prevention of Alzheimer's Dementia (EPAD) multicenter study [25]. EPAD general inclusion criteria were age above 50 years and no diagnosis of dementia (clinical dementia rating [CDR] score < 1). Exclusion criteria were the presence of conditions associated with neurodegeneration or affecting cognition, contraindication to MRI or lumbar puncture, and cancer or history of cancer in the preceding 5 years [24]. For this work, we selected participants who had CSF $A\beta_{1-42}$ and p-Tau_{181} measurements available, full genotyping, as well as structural and diffusion MRI, resulting in a final sample of 803 participants.

Genetic data processing and risk scores calculation

DNA samples were genotyped using Illumina Infinium Global Screening Array-24 v3.0. Standard quality control pipelines were applied using PLINK (www.cog-genomics.org) and are available online (https://github.com/marioni-group/epad-gwas). Briefly, quality control ensured high-quality genotypes in all individuals (individual call rate > 99%, variant call rate > 99%), excluding single nucleotide polymorphisms (SNPs) with a significant departure from Hardy–Weinberg equilibrium ($p < 1 \times 10$) and keeping SNPs with minor allele frequency > 0.5%. Before imputation, individuals of non-European ancestry ($n = 19$, based on clustering with HapMap III reference data) and individuals with a family relation ($n = 46$, identity-by-descent > 0.1875) were excluded.

Genotypes were imputed using the Michigan Imputation Server (https://imputationserver.sph.umich.edu) [26] against European sample data from the Haplotype Reference Consortium (HRC, v1.1, GRCh37). Analyses were restricted to SNPs with imputation quality scores (RSq) ≥ 0.6 and minor allele frequencies (MAFs) ≥ 0.0005. More details about genetic data acquisition and processing procedures are documented in previous works [10]. PRSs were constructed using 85 genome-wide significant variants identified in the most recent genome-wide association study (GWAS) of AD and related dementias [8], performed in a sample of individuals that had no overlap with the EPAD cohort. The variant effect-sizes (log of odds ratio) reported in the original work (Supplementary Table 1) were used as weights for the PRSs. PRSs were computed as the summation of risk alleles carried, weighted by their effect sizes from the reference GWAS, for each individual. To investigate the effects of genetic variants beyond *APOE*, PRSs were computed both with and without the two alleles (rs7412 and rs429358) from the *APOE* gene (denoted as *APOE*-PRS and *noAPOE*-PRS, respectively).

Pathway-specific PRSs

We then computed PRSs related to specific biological pathways, using a previously developed data-driven method [27]. Method description and validation in EPAD can be found in previous works [10]. Briefly, each of the selected SNPs (excluding the *APOE* region) was first annotated to a candidate gene in line with the variant-gene mapping performed in the original GWAS work, thus integrating variant annotation, quantitative-trait-loci (QTL) (such as expression-QTL, protein-QTL, splicing-QTL, methylation-QTL, histone acetylation-QTL), and APP metabolism procedures. Detailed information about the annotation procedure is reported in the original work [8]. Prioritized genes are reported in Supplementary Table 1. Subsequently, we mapped genes to biological pathways of interest using snpXplorer [27]. The *Gost* function from the R package gprofiler2 [28] was used with Gene Ontology [29] as a reference source for gene-sets. After gene-set enrichment analysis, snpXplorer calculates a semantic similarity matrix (based on Lin distance) [30] between all enriched pathways, which is then used in a hierarchical clustering framework to obtain clusters of similar pathways. By counting the number of times each SNP was associated with each cluster of pathways and dividing by the total number of associations per SNP, we obtained a weighted mapping factor of each SNP to each cluster of pathways, varying between 0 and 1 and reflecting the contribution of that SNP to that cluster of pathways. In case no mapping to any of the pathways was found, we excluded the SNP from further analyses. Given this weighting factor, pathway-specific PRSs were computed as an extended definition of the global PRS, by adding as a multiplicative factor the variant-pathway-mapping weight of each variant, and thus obtaining N pathway-specific PRSs estimates per subject, with N being the number of identified clusters. The resulting clusters were the immune activation, signal transduction, inflammation, lipid, amyloid, and clearance pathways.

CSF analysis

CSF biomarkers were quantified using a harmonized pre-analytical protocol. Analyses were performed with the fully automatised Roche cobas Elecsys System at the Clinical Neurochemistry Laboratory, Mölndal, Sweden [24]. Concentrations of $A\beta_{1-42}$ were determined using

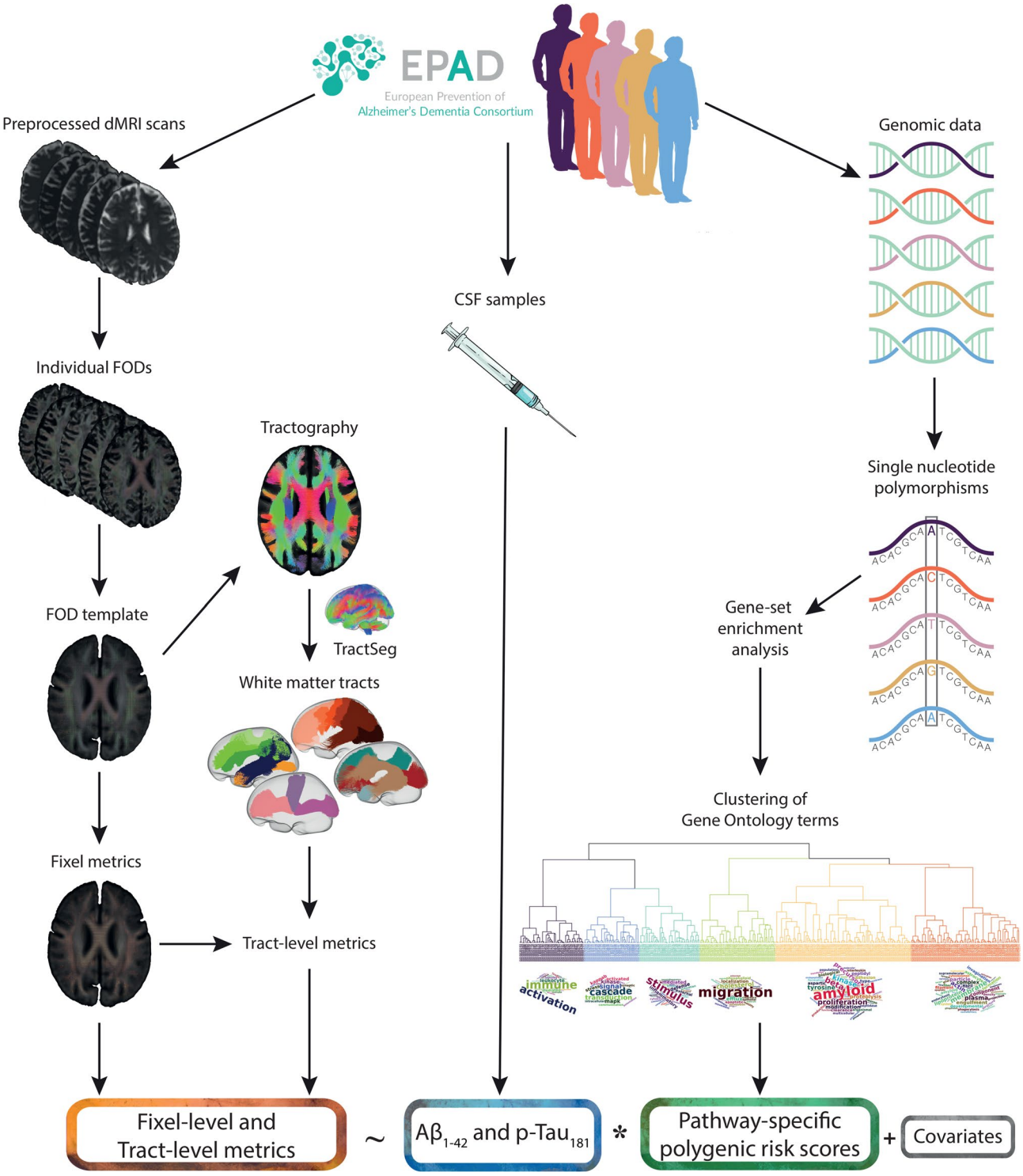

Fig. 1 Study workflow. MRI, CSF and genomic data were obtained from the pan-European EPAD cohort. *Abbreviations*: dMRI = diffusion MRI; FOD = fiber orientation distribution; CSF = cerebrospinal fluid; EPAD = European Prevention of Alzheimer's Dementia

the manufacturer's guidelines. Following previous studies on the same cohort [31], CSF $A\beta_{1-42}$ levels < 1000 pg/mL were used to define $A\beta_{1-42}$ positivity (A+), and CSF p-Tau_{181} levels > 27 pg/mL were used to define p-Tau_{181} positivity (T+). Since A-T + individuals are not considered to have AD-related pathophysiological changes [4], they were excluded from further analysis.

MRI acquisition and processing

MRI acquisition details have been reported elsewhere [32]. Diffusion weighted images (DWI, voxel size = 2.0 × 2.0 × 2.0 mm^3, diffusion-encoding directions = 30, 2 b-values = b0 and b1000 s/mm2) were processed using QSIPrep 0.19.0 [33], including denoising, B1 field inhomogeneity correction, head motion, eddy current and susceptibility distortion correction. Further processing steps were carried out using commands implemented within MRtrix3 (www.mrtrix.org). Specifically, DWI images were upsampled to a voxel size of 1.25 mm^2 using cubic b-spline interpolation. Group-averaged response functions for WM, gray matter and CSF were used to compute fiber orientation distributions (FOD) with single-shell 3-tissue constrained spherical deconvolution [34]. Subsequently, joint bias field correction and intensity normalization were performed [35, 36]. Through an interactive registration and averaging approach, a group template image was generated using WM FOD images from a subset of 36 subjects chosen to be representative of the study population and proportionally sampled from each site [37]. Spatial correspondence was achieved by registering all subject-level FOD to the template via FOD-guided nonlinear registration [37, 38]. Probabilistic tractography was then applied to the group template to generate a whole-brain tractogram with 20 million streamlines, that were filtered to 2 million streamlines using SIFT (spherical-deconvolution informed filtering of tractograms) to reduce reconstruction biases [39]. By applying the fixel-based analysis framework, measures of FD and log-FC (hereafter referred to as FC) were obtained at each WM fixel in group template space for all subjects [19] and connectivity-based smoothed [40]. Briefly, FD depicts changes in the volume of restricted water within a given fixel, while FC describes the local expansion or contraction in the plane perpendicular to the fiber orientation. WM tracts were delineated on the group template using TractSeg [41], and converted into binary fixel masks, which were used to extract tract-level mean fixel measures for all participants. Tract-level values were harmonized across sites using ComBat to remove batch effects while preserving the effects of all variables included in our subsequent analyses [42]. Based on the literature [43], we included thirteen WM tracts: the arcuate fasciculus, the inferior and middle longitudinal fasciculi, the three subdivisions of the superior longitudinal fasciculus, the inferior fronto-occipital fasciculus, the uncinate fasciculus, the cingulum bundle, the anterior and superior thalamic radiations, the corpus callosum, and the optic radiation. Estimated total intracranial volume (eTIV) was obtained from 3D T1-weighted images using FreeSurfer v.7.1.1. WM lesion burden was computed from FLAIR images using the Bayesian model selection toolbox (BaMoS) [44].

Statistical analysis

Linear regression models were used to assess the association between AD-related pathophysiological changes (i.e., CSF concentrations of $A\beta_{1-42}$ and p-Tau_{181}), genetic risk and WM integrity (i.e., FD and FC) at the tract-level. Models were adjusted for confounding factors such as age, sex, log-eTIV (only for FC) [45], population substructure (using the first five genetic principal components), and *APOE*-ε4 carriership when testing the effect of *APOE*-independent PRSs (i.e., *noAPOE*-PRS and pathway-specific PRSs) and AD-related pathophysiological changes. The analyses were repeated, adjusting for WM lesion burden, years of education, handedness and CDR score. In addition, we performed stratified analyses within CDR groups. Interaction analyses were performed to determine whether PRSs moderated the relationship between AD-related pathophysiological changes and WM integrity. $A\beta_{1-42}$ and p-Tau_{181}were entered into the models as continuous variables and were used to stratify the population into A + and T + groups for visualization purposes only. *P*-values were corrected for multiple comparisons using the false discovery rate (FDR) method and considered significant when pFDR ≤ 0.05. Only for the significant associations, we explored the spatial distribution of the effects at the fixel-level using the same models. In these fixel-level models, statistical inference was performed using connectivity-based fixel enhancement (CFE) based on tractography informed fixel-to-fixel connectivity. Fixels below the 5th percentile of extent of fixel-to-fixel connectivity were excluded from the analysis. Significance of each fixel was assessed with the family-wise error (FWE) method using non-parametric permutation testing over 5000 permutations. Analyses were performed using R studio (v 4.4.0).

Results

Cohort characteristics

The study population included 803 participants (Table 1). The mean age was 64.7 (± 7.3) years, 458 (57.0%) were females, 275 (34.2%) were *APOE*-ε4 carriers, and 185 (23%) had a global CDR score of 0.5.

Table 1 Clinical and demographic characteristics of the study population

	N **= 803**
Age (years)	64.7 (7.3)
Sex [females, *n* (%)]	458 (57.0%)
CDR global score = 0.5 [*n* (%)]	185 (23.0%)
Years of education	14.3 (3.8)
APOE -ε4 carriers [*n* (%)]	275 (34.2%)
A+ [*n* (%)]	291 (36.2%)
CSF $A\beta_{1-42}$ (pg/mL)	1320.1 (620.8)
T+ [n (%)]	71 (8.8%)
CSF p-Tau_{181} (pg/mL)	17.9 (8.3)
eTIV (mL)	1501.0 (160.0)
Handedness [right-handed, *n* (%)]	760 (94.6%)
WMH volume (mL)	5.4 (6.2)

Data are expressed as mean ± standard deviation, unless otherwise specified. CSF $A\beta_{1-42}$ levels < 1000 pg/mL were used to define A+, and CSF p-Tau_{181} levels > 27 pg/mL were used to define T+

Abbreviations: *CDR* clinical dementia rating, *CSF* cerebrospinal fluid, *eTIV* estimated total intracranial volume, *WMH* white matter hyperintensities

Association between AD-related pathophysiological changes and WM properties

P-Tau_{181} was associated with greater FD in most of the analyzed tracts, including the corpus callosum ($\beta = 0.19$, $p_{FDR}<0.001$), projection fibers of the anterior thalamic ($\beta = 0.20$, $p_{FDR}<0.001$) and optic radiation ($\beta = 0.21$, $p_{FDR}<0.001$), and associative fibers of the arcuate ($\beta = 0.14$, $p_{FDR}=0.006$), inferior longitudinal ($\beta = 0.18$, $p_{FDR}<0.001$), middle longitudinal ($\beta = 0.19$, $p_{FDR}<0.001$), superior longitudinal II ($\beta = 0.11$, $p_{FDR}=0.04$), and inferior fronto-occipital fasciculus ($\beta = 0.18$, $p_{FDR}<0.001$) (Fig. 2A). At the fixel-level, this association was corroborated, with widespread effects observed in the corpus callosum and predominantly left-lateralized effects in projection fibers of the anterior thalamic and optic radiation, and associative fibers of the inferior longitudinal, middle longitudinal and inferior fronto-occipital fasciculus (Fig. 2B). Few effects in the opposite direction (i.e., lower FD with higher p-Tau_{181}) were also observed in the corpus callosum and anterior thalamic radiation (Fig. 2C). No associations between $A\beta_{1-42}$ and FD, or between either $A\beta_{1-42}$ or p-Tau_{181} and FC emerged. Directionality of effects was confirmed when correcting for WM lesion burden, years of education, handedness and CDR score (Supplementary Fig. 1). When analyzing CDR groups in isolation, we observed that directionality of effects was consistent across both groups (Supplementary Fig. 2).

Association between PRSs and WM properties

The *APOE*-PRS and *noAPOE*-PRS were both associated with greater FD of the superior longitudinal fasciculus I ($\beta = 0.16$, $p_{FDR}=0.017$ and $\beta = 0.13$, $p_{FDR}=0.003$, respectively) and superior longitudinal fasciculus II ($\beta = 0.14$, $p_{FDR}=0.04$ and $\beta = 0.10$, $p_{FDR}=0.02$, respectively). The identified pathway-specific PRSs included the immune activation, signal transduction, inflammation, lipid, amyloid and clearance pathways. Among these, the lipid pathway exhibited distributed positive effects on FD in associative fibers, comprising the arcuate ($\beta = 0.09$, $p_{FDR}=0.04$), superior longitudinal I ($\beta = 0.12$, $p_{FDR}=0.01$), superior longitudinal II ($\beta = 0.10$, $p_{FDR}=0.03$), middle longitudinal ($\beta = 0.08$, $p_{FDR}=0.048$), and inferior longitudinal fasciculus ($\beta = 0.08$, $p_{FDR}=0.048$) (Fig. 3A). The amyloid pathway was associated with greater FD of the superior longitudinal fasciculus I ($\beta = 0.12$, $p_{FDR}=0.01$).

The lipid pathway also showed a positive association with FC in most of the explored tracts (Fig. 3B), comprising the corpus callosum ($\beta = 0.06$, $p_{FDR}=0.004$), projection fibers of the superior thalamic ($\beta = 0.06$, $p_{FDR}=0.03$), anterior thalamic ($\beta = 0.05$, $p_{FDR}=0.01$) and optic radiation ($\beta = 0.05$, $p_{FDR}=0.04$), as well as associative fibers of the arcuate ($\beta = 0.04$, $p_{FDR}=0.04$), inferior fronto-occipital ($\beta = 0.04$, $p_{FDR}=0.03$), superior longitudinal I ($\beta = 0.07$, $p_{FDR}=0.01$), superior longitudinal II ($\beta = 0.08$, $p_{FDR}=0.004$) and superior longitudinal fasciculus III ($\beta = 0.05$, $p_{FDR}=0.04$), and of the cingulum bundle ($\beta = 0.06$, $p_{FDR}=0.001$). The association between the lipid pathway and greater FC was corroborated at the fixel-level in the corpus callosum, anterior thalamic radiation, and associative fibers of the arcuate fasciculus, superior longitudinal fasciculus I and II. These effects were mainly lateralized in the left hemisphere (Fig. 3C). Directionality of effects was confirmed when correcting for WM lesion burden, years of education, handedness and CDR score (Supplementary Figs. 3 and 4). Additionally, directionality of effects was consistent across CDR groups (Supplementary Figs. 5 and 6).

PRSs moderate the association between AD-related pathophysiological changes and WM properties

The *APOE*-PRS ($p_{FDR}=0.02$), the *noAPOE*-PRS ($p_{FDR}=0.01$), and the clearance pathway ($p_{FDR}=0.045$) significantly moderated the association of $A\beta_{1-42}$ with FD of the inferior longitudinal fasciculus. Specifically, the A + individuals showed positive associations between FD and the *APOE*-PRS, the *noAPOE*-PRS and the clearance pathway compared to A- ($\beta = 0.24$ *versus* $\beta = -0.01$, $\beta = 0.18$ *versus* $\beta = -0.04$, and $\beta = 0.12$ *versus* $\beta = -0.04$, respectively) (Fig. 4A-B). At the fixel-level, the moderation of the clearance pathway on the relationship between $A\beta_{1-42}$ and FD was mainly lateralized in the left hemisphere (Fig. 4C). The immune activation pathway significantly moderated the association of p-Tau_{181} with FD of the inferior fronto-occipital fasciculus ($p_{FDR}=0.04$), inferior longitudinal fasciculus ($p_{FDR}=0.04$), and optic radiation ($p_{FDR}=0.04$), with negative slopes exclusively in T + compared to T- individuals ($\beta = -0.35$ *versus* $\beta = 0.01$, $\beta = -0.26$ *versus* $\beta = 0.01$, and $\beta = -0.26$ *versus* $\beta = 0.03$, respectively) (Fig. 5A-B).

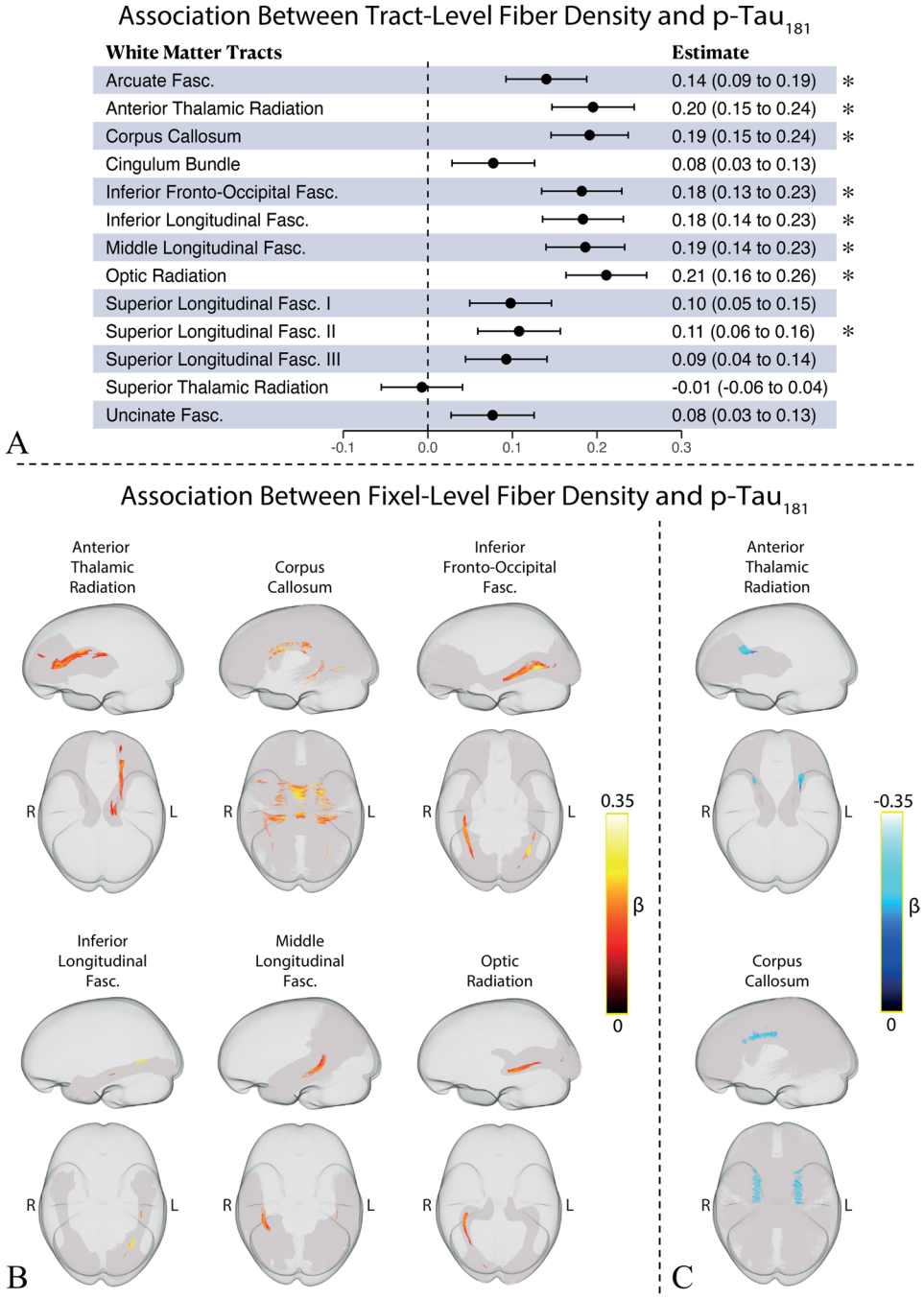

Fig. 2 Association between p-Tau$_{181}$ and white matter fiber density. (**A**) Forest plot showing that p-Tau181 was associated with greater tract-level fiber density in most analyzed tracts. (**B**) This relationship was largely corroborated at the fixel-level, with (**C**) some associations observed in the opposite direction. Significant associations in panel **A** are marked with an asterisk. *Abbreviations*: Fasc. = fasciculus; L = left; R = right

Discussion

We investigated the effect of AD-related pathophysiological changes, pathway-specific PRSs and their interaction on WM micro- and macrostructural integrity (at the tract and fixel levels) by leveraging diffusion MRI, CSF quantification of Aβ_{1-42} and p-Tau$_{181}$, and genomic data from a large multicentric cohort of non-demented older adults. No associations were observed between Aβ_{1-42} concentrations and WM fiber properties. Conversely, p-Tau$_{181}$ levels were mainly positively associated with FD, although some WM tracts exhibited coexisting patterns of negative associations, suggesting a multiphasic relationship. Among the pathway-specific PRSs, the lipid pathway demonstrated widespread positive associations with both FD and FC. Pathway-specific PRSs significantly moderated the association between

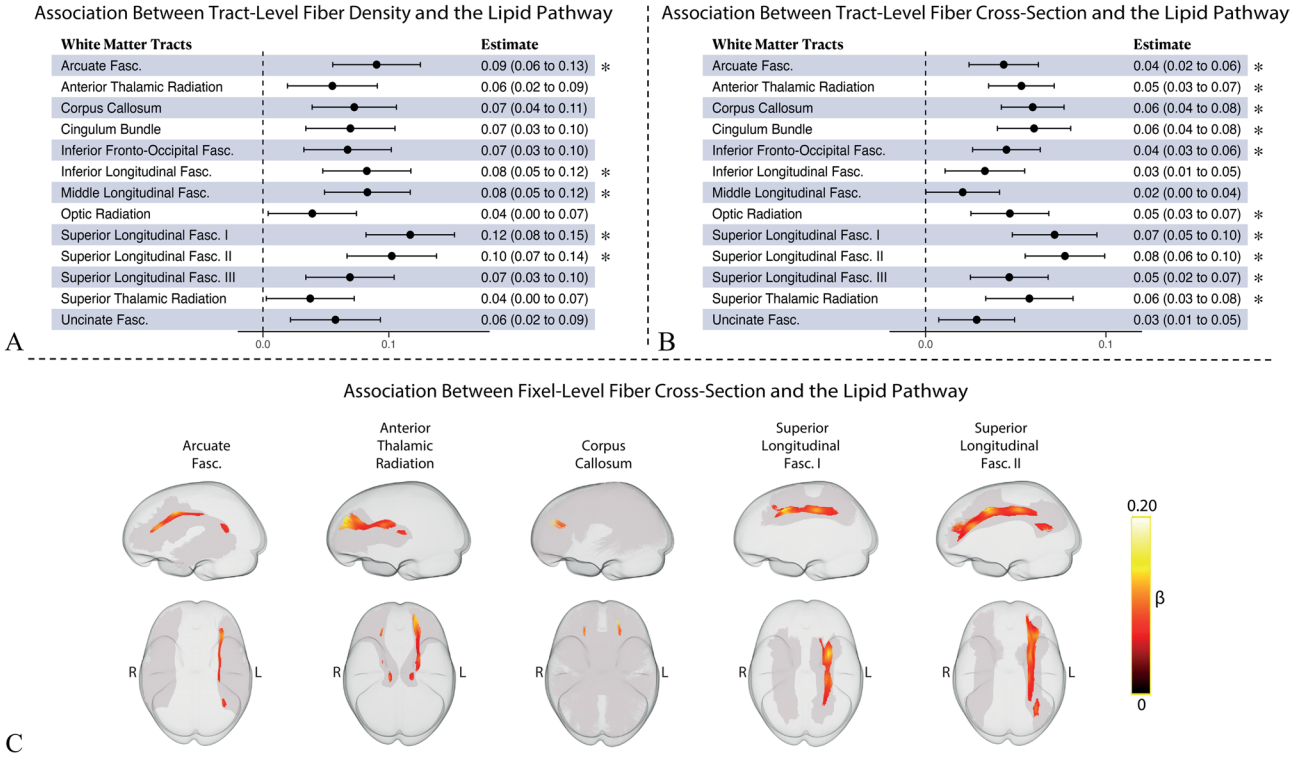

Fig. 3 Association between the lipid pathway and white matter fiber density and cross-section. Forest plots showing that the lipid pathway was associated with greater tract-level fiber density (**A**) and cross-section (**B**) in most analyzed tracts. (**C**) At the fixel-level, the association with greater fiber cross-section was mainly lateralized in the left hemisphere. Significant associations in panels **A** and **B** are marked with an asterisk. *Abbreviations*: Fasc. = fasciculus; L = left; R = right

AD-related pathophysiological changes and WM fibers integrity. Specifically, the clearance pathway moderated the relationship between $A\beta_{1-42}$ and FD, with increasing effects observed only in A + individuals, while the immune activation pathway moderated the association between p-Tau_{181} and FD, showing decreases exclusively in T + individuals. Overall, our findings indicate that polygenic risk linked to distinct biological pathways is associated with WM integrity both directly and by moderating the effect of established proteinopathy, highlighting the role of individual genetic vulnerability in shaping the brain's response to AD-related pathophysiological changes and offering insights for early patient stratification and management.

Our observations align with previous evidence showing no association between $A\beta_{1-42}$ and WM properties as assessed with the FBA framework in early stages of AD [21, 22]. In more advanced stages, however, a negative relationship between $A\beta_{1-42}$ and fixel metrics has been reported [20, 23]. While these discrepancies may partly stem from differences in statistical approaches and inclusion criteria, it is also possible that the observed associations were driven by cognitive status instead. Indeed, WM alterations have been linked to cognitive impairment even in the absence of correlations with $A\beta_{1-42}$ [21, 22]. This further supports the notion that $A\beta_{1-42}$ does not independently affect WM integrity and that other factors play a moderating role in disease progression [6]. On the other hand, while previous studies found either no effects of p-Tau_{181} [20], or reported effects restricted to lower FC in limbic tracts [22, 23], we found associations of p-Tau_{181} with widespread alterations in FD. Our study focused on non-demented (and predominantly cognitively unimpaired) older adults. This supports the idea that FD is more sensitive to early proteinopathy than FC, aligning with established evidence that neurodegeneration occurs later in the disease continuum, with FC reflecting macrostructural changes (i.e., atrophy) [46]. Interestingly, p-Tau_{181} was predominantly associated with greater FD, challenging the traditional view of p-Tau_{181} as primarily linked to degeneration and offering new insights into its early effects on WM. This could be explained by emerging evidence that p-Tau_{181} propagates both through and along synaptic connections, facilitated by intra- and extracellular vesicles, respectively [47, 48]. Since these processes precede synaptic loss [47], an initial increase in local density, which then is still unopposed by neurodegenerative changes, may manifest as apparent greater FD in a largely cognitively preserved population. However, as our findings are based on cross-sectional data, and given evidence that p-Tau_{181} spreads between structurally connected brain regions [49], we cannot rule out

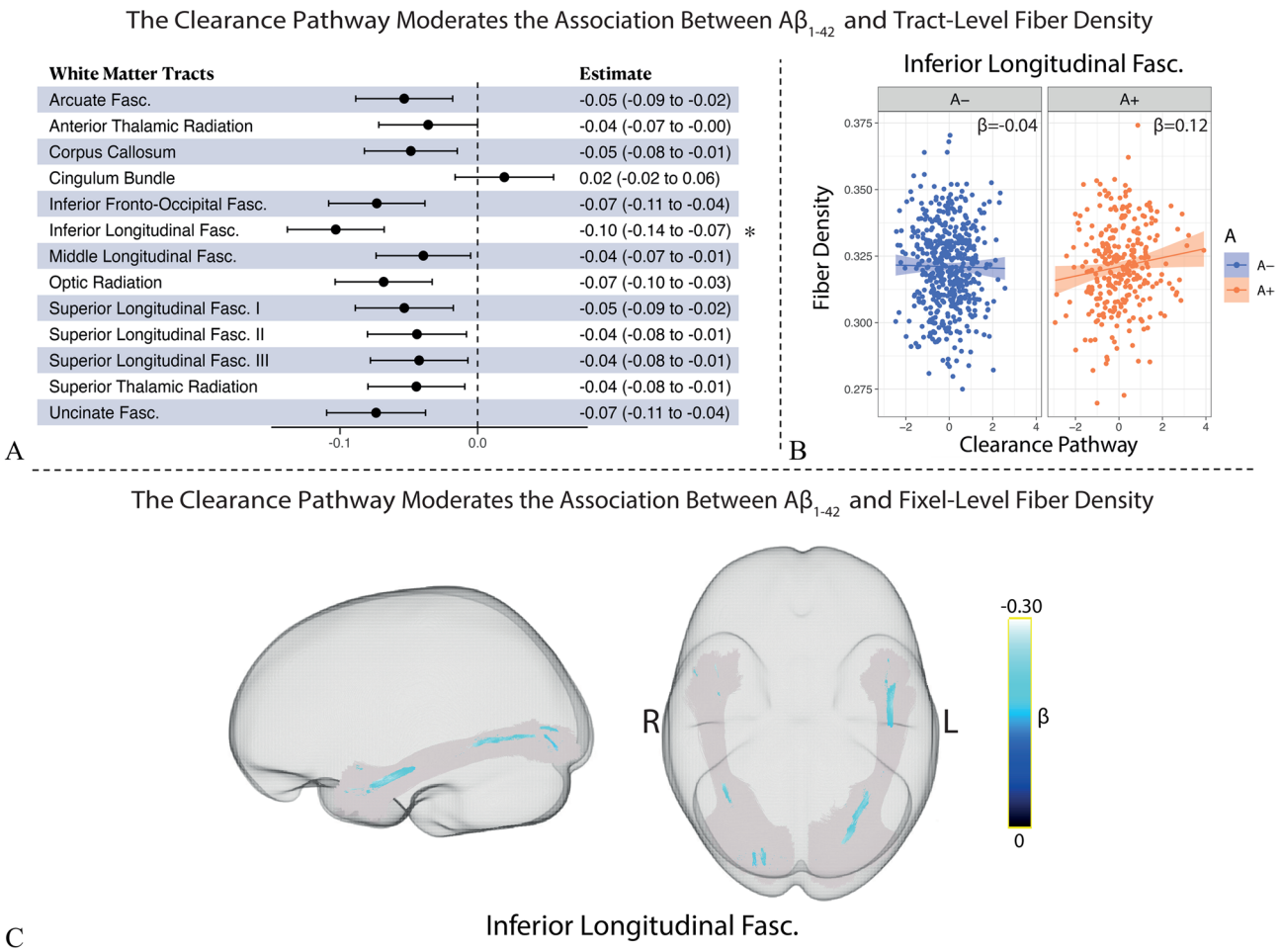

Fig. 4 The clearance pathway moderates the association between $A\beta_{1-42}$ and white matter fiber density. (**A**) Forest plot showing that the clearance pathway significantly moderated the effect of $A\beta_{1-42}$ on tract-level fiber density of the inferior longitudinal fasciculus. (**B**) Scatterplot showing increased tract-level fiber density with higher genetic risk related to the clearance pathway, exclusively in A + participants. (**C**) Fixel-level distribution of the moderation effect. Significant associations in panel **A** are marked with an asterisk. *Abbreviations*: Fasc. = fasciculus; L = left; R = right

the possibility that greater FD facilitates the propagation of protein misfolding, leading to increased p-Tau_{181}. Furthermore, the coexistence of increased and decreased FD in relation to p-Tau_{181} suggests a non-linear, multiphasic relationship, wherein WM degeneration occurs only after p-Tau_{181} surpasses a certain threshold, as supported by previous evidence based on diffusion tensor imaging [50]. The progressive accumulation of hyperphosphorylated tau has been linked to loss of microtubule stability, impaired axonal transport and necroptosis [51, 52], which eventually lead to WM degeneration through axonal retraction and secondary Wallerian degeneration [53, 54]. Longitudinal studies are warranted to clarify these aspects and establish a potential causal relationship.

Our findings suggest that the lipid pathway, which involves genes related to cholesterol metabolism and membrane integrity, plays a crucial role in influencing both FD and FC, highlighting its potential as a critical biological mechanism in AD-related white matter changes. Dysfunction in this biological pathway has already been associated with increased and defective myelin production and turnover [13, 14]. Excessive cholesterol concentration dysregulates myelin growth [55], resulting in the aberrant production of redundant myelin (i.e., myelin outfolding) [56]. Additionally, it impairs the efficient removal of myelin debris, leading to the accumulation of multilamellar fragments, which ultimately exacerbates amyloid plaques formation [56, 57]. In this light, our results suggest that individual genetic susceptibility to these processes is linked to deficiencies in WM tract remodeling, and that these alterations can be captured using fixel-based metrics. Defective myelin sheaths are more vulnerable to age-related myelin breakdown, which, in turn, triggers the production of $A\beta_{1-42}$ and p-Tau_{181} as a homeostatic response, fostering a vicious cycle that has been described as the progressive "Alzheimerization" of the aging brain [13]. Notably, the observed effects were exclusively located in the left hemisphere in the arcuate

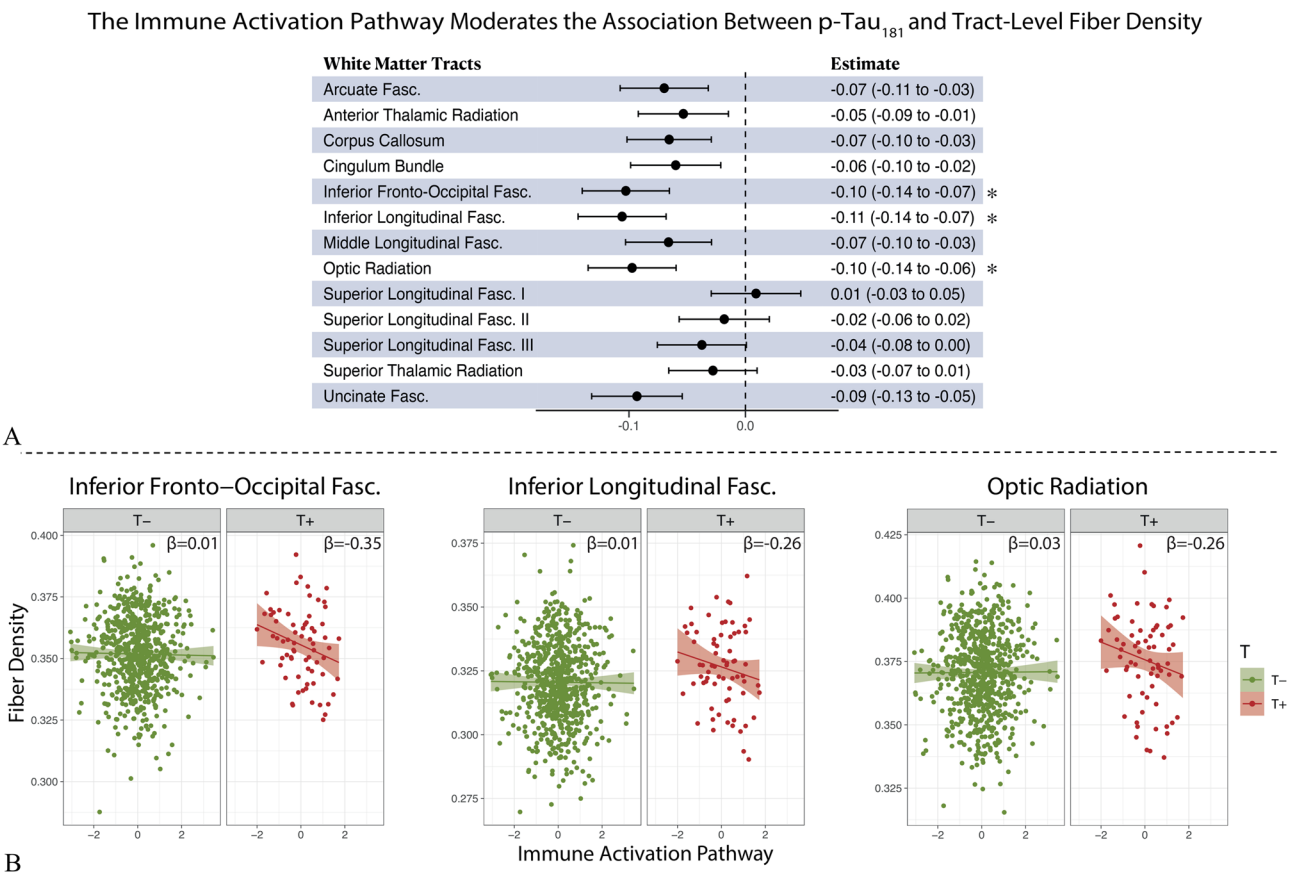

Fig. 5 The immune activation pathway moderates the association between p-Tau$_{181}$ and white matter fiber density. (**A**) Forest plot showing that the immune activation pathway significantly moderated the effect of p-Tau$_{181}$ on tract-level fiber density of the inferior fronto-occipital fasciculus, inferior longitudinal fasciculus and optic radiation. (**B**) Scatterplots showing decreased tract-level fiber density with higher genetic risk related to the immune activation pathway, exclusively in T + participants. Significant associations in panel **A** are marked with an asterisk. *Abbreviations*: Fasc. = fasciculus

fasciculus and superior longitudinal fasciculus I and II. Alterations in these tracts have already been described in relation to AD [20, 58], along with functional impairment in the connecting frontal, parietal and temporal brain regions [59]. The lateralized effects aligns with well-established evidence on the hub architecture of the human brain, where hub regions are more strongly interconnected, and therefore exhibit greater metabolic demands and heightened vulnerability to neural insults [60], such as pathological proteins spreading and accumulation [61]. Lateralization of effects was further confirmed by correcting for handedness. However, while our findings align with previous evidence showing that the left predominance of these WM tracts is independent from age, sex and handedness [62, 63], the high prevalence of right-handed individuals in our sample (n = 760, 94.6%) highlights the need for further studies to determine whether these effects are truly independent of handedness and whether left-handed individuals exhibit right-lateralized effects.

Finally, we demonstrated that genetic risk factors interact with AD-related pathophysiological changes to shape WM vulnerability. These interactions provide evidence that specific biological processes are activated in response to proteinopathy, ultimately driving WM alterations. Specifically, we found that the clearance pathway, including genes responsible for tissue homeostasis, significantly moderated the association between Aβ_{1-42} and greater FD in the inferior longitudinal fasciculus. Impaired tissue homeostasis, on a substrate of greater tissue density, likely facilitates the accumulation of cellular debris, leading to a buildup of neurotoxic molecules that further impair local clearance and promote the formation of amyloid plaques [13]. While FBA proved sensitive to these associations, future mechanistic studies incorporating FBA-derived metrics will be essential to fully interpret these findings. Similarly, the immune activation pathway moderated the negative relationship between p-Tau$_{181}$ and FD exclusively. The preferential colocalization of activated immune cells with p-Tau$_{181}$ compared to Aβ_{1-42} has been proved in vivo using inflammation PET tracers [64], and supports the idea that p-Tau$_{181}$ deposition is the main factor eliciting the immune response and ultimately leading to neurodegenerative changes,

also in non-demented adults [65]. From an anatomical standpoint, the particular sensitivity of the inferior longitudinal fasciculus, where these associations were both detectable, likely stems from its connection to regions within the default mode network, whose alterations are associated with early pathological and clinical changes in AD [66]. Neurobiologically, these findings align with recent research showing that genetic risk contributes differently to disease progression at various stages of AD [11] and reinforce long-standing evidence that AD pathological changes do not fully explain disease stage - an observation that led to the postulation of "brain reserve" as a key factor in individual resilience [67]. In line with evidence that biological and clinical heterogeneity along the AD continuum is linked to genetic variability [68, 69], our observations advocate for the integration of genomic information alongside $A\beta_{1-42}$ and p-Tau_{181}, into the conceptual framework of AD staging. This integrated, personalized perspective on the temporal evolution of AD could help guide targeted screening and intervention strategies in future preclinical trials aimed at specific biological pathways.

Our study comes with a number of limitations. Firstly, our findings are based on a cohort of non-demented older adults, therefore generalization to diverse populations or clinical stages of AD requires further investigation. Secondly, while pathways-PRSs and their interaction with AD-related pathophysiological changes are linked to WM alterations, mechanistic studies are needed to elucidate the precise biological processes driving these effects. As our findings are based on cross-sectional data, future longitudinal research should track the observed WM alterations over time. Notably, results were replicated when correcting for CDR. However, when analyzing CDR groups separately, the same directionality of effects was observed in both groups, but uncertainty increased, particularly among participants with CDR > 0, who were underrepresented in our sample. Further studies including individuals across a broader spectrum of disease severity are needed to clarify how cognitive deterioration influences the relationship between genetic risk and structural alterations along the disease trajectory. In the present study, we focused on p-Tau_{181} due to the unavailability of alternative epitopes at the time of EPAD data collection. While different p-Tau epitopes may capture distinct aspects of AD pathology, they are generally highly correlated and provide partially overlapping information [1]. For instance, p-Tau_{231} (in plasma) correlates strongly with amyloid plaques but less with tau tangles compared to p-Tau_{181} and p-Tau_{217} [70]. Therefore, while p-Tau_{231} is highly sensitive to early amyloid-related changes, including both $A\beta_{1-42}$ and p-Tau_{181} provides complementary information on early disease trajectories, capturing distinct pathological processes. Further studies are needed to systematically compare the sensitivity of different p-Tau epitopes. Moreover, the recent availability of additional p-Tau epitopes that more closely reflect tau tangle pathology, such as p-Tau_{217}, p-Tau_{205}, and MTBR-tau_{243} [70–72], warrants future studies including these markers to enable a more nuanced characterization of stage-specific pathological changes and to refine interpretations in preclinical or early AD stages. Additionally, further studies are needed to validate our findings using PET and investigate whether environmental and lifestyle factors may moderate the relationship between genetic risk, AD-related pathophysiological changes, and WM integrity. It is noteworthy that, consistent with prior genetic research, the observed effect sizes for the pathway-specific PRSs were modest yet biologically meaningful. Aggregating multiple alleles highlights convergence on cellular and molecular pathways implicated in AD pathophysiology, even in the absence of *APOE* [9]. From a clinical perspective, PRSs have been shown to be significantly associated with AD and to discriminate between AD and healthy controls [73]. Their predictive ability for cognitive decline, however, has been inconsistent [73]. While *APOE*-ε4 remains the strongest single predictor, the inclusion of pathway-specific PRSs improves prediction accuracy beyond *APOE*-ε4 alone, capturing additional information [73]. Thus, although the individual effects of *APOE*-independent PRSs are small, they hold promise for risk stratification and for informing pathway-targeted early interventions. Lastly, while we applied multiple comparisons correction to minimize the risk of spurious findings, we acknowledge that the results may not be easily generalizable to the broader population. This limitation reflects both technical factors (e.g., the use of advanced MRI metrics and pathway-specific PRSs that are not yet widely available) and biological factors, including the substantial heterogeneity observed across the AD spectrum. Nonetheless, our findings highlight the potential value of integrating genetic data into the AD diagnostic framework to identify individuals most vulnerable to AD-related pathophysiological changes, and they underscore the need for replication in diverse populations and across different disease stages to support clinical translatability.

Conclusions

In conclusion, we demonstrated that polygenic risk for AD influences WM integrity both directly and by moderating the effect of established AD proteinopathy. The role of individual genetic vulnerability in driving the brain's response to AD pathological alterations must be integrated in the AD diagnostic framework to enable informed screening and intervention for future preclinical trials targeting specific biological pathways.

Supplementary Information

The online version contains supplementary material available at https://doi.org/10.1186/s13195-025-01888-3.

Supplementary Material 1

Acknowledgements
We thank the study participants.

Authors' contributions
MT: Conceptualization; Analysis; Interpretation; Writing—original draft preparation. LP: Writing—review and editing; Analysis; Interpretation. GP: Writing—review and editing; Analysis. ESL: Writing—review and editing. LEC: Writing—review and editing. TGO: Writing—review and editing. NT: Writing—review and editing. NVT: Writing—review and editing. AA: Writing—review and editing. LR: Writing—review and editing. MP: Writing—review and editing. HH: Writing—review and editing. MR: Writing—review and editing. PP: Writing—review and editing; Data acquisition. PML: Writing—review and editing; Data acquisition. CWR: Writing—review and editing; Data acquisition. AW: Writing—review and editing; Data acquisition. JMW: Writing—review and editing. JDG: Writing—review and editing. GS: Writing—review and editing. AB: Writing—review and editing. HJMM: Writing—review and editing. AMW: Writing—review and editing. FB: Writing—review and editing; Supervision; Interpretation; Data acquisition. LL: Conceptualization; Writing—review and editing; Supervision; Analysis; Data acquisition. All authors read and approved the final manuscript.

Funding
This work was funded by EU/EFPIA Innovative Medicines Initiative (IMI) grant 115736; Horizon 2020 grant 115952. ESL has received support for data curation and storage from the Alzheimer's Disease Data Initiative (ADDI; paid to institution). LEC's salary is supported by a MSCA postdoctoral fellowship research grant (101108819) and the Alzheimer Association Research Fellowship (grant 23AARF-1029663). NV-T is supported by the Spanish Ministry of Science and Innovation - State Research Agency grant RYC2022-038136-I, cofunded by the European Union FSE+, and grant PID2022-143106OA-I00 cofunded by the European Union FEDER; NV-T is supported by the William H. Gates Sr. Fellowship from the Alzheimer's Disease Data Initiative, and grant 23S06083-001 funded by the Ajuntament de Barcelona and "la Caixa" Foundation. AA was supported by the Early Detection of Alzheimer's Disease Subtypes (E-DADS) project, an EU Joint Programme—Neurodegenerative Disease Research (JPND) project (see www.jpnd.eu). JMW is supported by the UK Dementia Research Institute (funded by the MRC, Alzheimer's Society and Alzheimer's Research UK), the British Heart Foundation, The Fondation Leducq Network on Perivascular Spaces and the Row Fogo Centre for Research into Small Vessel Diseases. HJMMM is supported by the Dutch Heart Foundation (03-004-2020-T049), by the Eurostars-2 joint programme with co-funding from the European Union Horizon 2020 research and innovation programme (ASPIRE E!113701), provided by the Netherlands Enterprise Agency (RvO), and by the EU Joint Program for Neurodegenerative Disease Research, provided by the Netherlands Organisation for health Research and Development and Alzheimer Nederland (DEBBIE JPND2020-568-106). LL receives funding from the MSCA postdoctoral fellowship (#101204296).

Data availability
Raw and processed data can be accessed from the EPAD website (http:/www.ep-ad.org) upon request.

Declarations

Ethics approval and consent to participate
The study was approved by the ethical committees of all participating centers. All study participants provided written informed consent according to the Declaration of Helsinki.

Competing interests
LEC has received research support from GE HealthCare and Springer Healthcare (funded by Eli Lilly), both paid to the institution. TGO has been a consultant for Sonae and Guidepoint, has received fees as a speaker from Eisai and conference fees covered from Roche and Lilly. JDG has received research support from GE HealthCare, Roche Diagnostics, and F. Hoffmann–La Roche; has received speaker or consulting fees from Roche Diagnostics, Esteve, Philips Nederlands, Biogen, and Life Molecular Imaging; and serves on the Molecular Neuroimaging Advisory Board of Prothena Biosciences. CWR has done paid consultancy work for Eli Lilly, Biogen, Actinogen, Brain Health Scotland, Roche, Roche Diagnostics, Novo Nordisk, Eisai, Signant, Merck, Alchemab, Sygnature, and Abbvie; his group has received Research Income to his Research Unit from Biogen, AC Immune and Roche; he has out licensed IP developed at University of Edinburgh to Linus Health and is CEO and Founder of Scottish Brain Sciences. FB is supported by the NIHR biomedical research center at UCLH. He has been a steering committee or Data Safety Monitoring Board member for Biogen, Merck, Eisai, and Prothena; an advisory board member for Combinostics and Scottish Brain Sciences; and a consultant for Roche, Celltrion, Rewind Therapeutics, Merck, and Bracco; FB has research agreements with ADDI, Merck, Biogen, GE HealthCare, and Roche and is a Cofounder and shareholder of Queen Square Analytics Ltd. The remaining authors have nothing to disclose.

Author details
[1]Department of Radiology and Nuclear Medicine, Amsterdam UMC location VUmc Amsterdam, De Boelelaan 1117, Amsterdam 1081 HV, Netherlands
[2]Department of Advanced Biomedical Sciences, University of Naples "Federico II", Via Pansini 5, Naples 80131, Italy
[3]Amsterdam Neuroscience, Brain Imaging, De Boelelaan 1085, Amsterdam 1081HV, Netherlands
[4]Department of Neuroinflammation, Queen Square Multiple Sclerosis Centre, UCL Queen Square Institute of Neurology, University College London, Queen Square, London WC1N 3BG, UK
[5]Department of Anatomy and Neurosciences, MS Center Amsterdam, Amsterdam Neuroscience, Amsterdam UMC , Vrije Universiteit Amsterdam, De Boelelaan 1117, Amsterdam 1081 HV, Netherlands
[6]Laboratory for Cognitive Neurology, Leuven Brain Institute, KU Leuven, ON5, Herestraat 49, Leuven 3001, Belgium
[7]Laboratory for Complex Genetics, KU Leuven, ON6, Herestraat 49, 610, Leuven, Belgium
[8]Department of Clinical Sciences, Clinical Memory Research Unit, Lund University, St Johannesgatan 8, Malmö 211 46, Sweden
[9]Life and Health Sciences Research Institute (ICVS), School of Medicine, University of Minho, Campus Gualtar, Braga 4710-057, Portugal
[10]ICVS/3B's - PT Government Associate Laboratory, Campus Gualtar, Braga, Guimarães 4710-057, Portugal
[11]Department of Neuroradiology, ULS/Hospital de Braga, Braga 4710-243, Portugal
[12]Genomics of Neurodegenerative Diseases and Aging, Human Genetics, Amsterdam UMC location VUmc, De Boelelaan 1117, Amsterdam 1081 HV, Netherlands
[13]Delft Bioinformatics Lab, Delft University of Technology, Van Mourik Broekmanweg 6, Delft 2628 XE, Netherlands
[14]BarcelonaBeta Brain Research Center (BBRC), Pasqual Maragall Foundation, Calle Wellington 30, Barcelona 08005, Spain
[15]Hospital del Mar Medical Research Institute, Doctor Aiguader 88, Barcelona 08003, Spain
[16]Centre for Genomic Regulation (CRG), Barcelona Institute of Science and Technology (BIST), Carrer del Doctor Aiguader, 88, Ciutat Vella, Barcelona 08003, Spain
[17]Department of Human Genetics, Radboud University Medical Center, Geert Grooteplein-Zuid 10, Nijmegen 6525 GA, Netherlands
[18]Department of Medical Physics, UCL Hawkes Institute, University College London, 90 High Holborn, London WC1E 6BT, UK
[19]IRCCS Ospedale Policlinico San Martino, Largo Rosanna Benzi 10, Genoa 16132, Italy
[20]Department of Health Sciences (DISSAL), University of Genoa, Via Antonio Pastore 1, Genoa 16132, Italy
[21]Department of Neuroscience, Rehabilitation, Ophthalmology, Genetics, Maternal and Child Health (DINOGMI), University of Genoa, Largo Paolo Daneo, 3, Genoa 16132, Italy
[22]Vlaams Instituut voor Biotechnologie Center for Brain and Disease Research, ON5, Herestraat 49, Leuven 3001, Belgium
[23]Department of Neurosciences, Leuven Brain Institute, KU Leuven, Onderwijs en Navorsing 5, Herestraat, box 1020, Leuven 3000, Belgium

[24]Department of Nuclear Medicine, Toulouse University Hospital, 2 Rue Charles Viguerie, Toulouse 31300, France
[25]Toulouse NeuroImaging Center, ToNIC, Inserm, UPS, University of Toulouse, Place du Dr Joseph Baylac, Toulouse 31024, France
[26]Centro de Investigación y Terapias Avanzadas, Neurología, CITA-Alzheimer Foundation, , Mikeletegi Pasealekua, 71, 1, Donostia, San Sebastián 20009, Spain
[27]Outpatient Department 2, Edinburgh Dementia Prevention, Centre for Clinical Brain Sciences, Western General Hospital, University of Edinburgh, Crewe Road South, Edinburgh EH4 2XU, UK
[28]Brain Health Scotland, 160 Dundee Street, Edinburgh EH11 1DQ, UK
[29]Centre for Clinical Brain Sciences, The University of Edinburgh, 49 Little France Crescent, Edinburgh EH16 4SB, UK
[30]Department of Medicine, Imperial College London, Ayrton Road, South Kensington, London SW7 5NH, UK
[31]UK Dementia Research Institute Centre at the University of Edinburgh, 49 Little France Crescent, Edinburgh EH16 4SB, UK
[32]Centro de Investigación Biomédica en Red Bioingeniería, Biomateriales y Nanomedicina, Instituto de Salud Carlos III, Monforte de Lemos, 3-5, Madrid 28029, Spain
[33]Centro Nacional de Investigaciones Cardiovasculares (CNIC), Calle Melchor Fernández Almagro 3, Madrid 28029, Spain
[34]Dementia Research Centre, UCL Queen Square Institute of Neurology, University College London, 8-11 Queen Square, London WC1N 3AR, UK

Received: 12 June 2025 / Accepted: 11 October 2025
Published online: 10 November 2025

References

1. Salvadó G, Horie K, Barthélemy NR, Vogel JW, Pichet Binette A, Chen CD, et al. Disease staging of Alzheimer's disease using a CSF-based biomarker model. Nat Aging. 2024;4:694–708. https://doi.org/10.1038/s43587-024-00599-y.
2. Coupé P, Manjón JV, Lanuza E, Catheline G. Lifespan changes of the human brain in Alzheimer's disease. Sci Rep. 2019;9:3998. https://doi.org/10.1038/s41598-019-39809-8.
3. Aisen PS, Jimenez-Maggiora GA, Rafii MS, Walter S, Raman R. Early-stage alzheimer disease: getting trial-ready. Nat Rev Neurol. 2022;18:389–99. https://doi.org/10.1038/s41582-022-00645-6.
4. Jack CR Jr, Andrews JS, Beach TG, Buracchio T, Dunn B, Graf A, et al. Revised criteria for diagnosis and staging of Alzheimer's disease: Alzheimer's association workgroup. Alzheimers Dement. 2024. https://doi.org/10.1002/alz.13859.
5. Brookmeyer R, Abdalla N. Estimation of lifetime risks of Alzheimer's disease dementia using biomarkers for preclinical disease. Alzheimers Dement. 2018;14:981–8. https://doi.org/10.1016/j.jalz.2018.03.005.
6. Villain N, Planche V. Disentangling clinical and biological trajectories of neurodegenerative diseases. Nat Rev Neurol. 2024;20:693–4. https://doi.org/10.1038/s41582-024-01004-3.
7. Karlsson IK, Escott-Price V, Gatz M, Hardy J, Pedersen NL, Shoai M, et al. Measuring heritable contributions to Alzheimer's disease: polygenic risk score analysis with twins. Brain Commun. 2022;4:fcab308. https://doi.org/10.1093/braincomms/fcab308.
8. Bellenguez C, Küçükali F, Jansen IE, Kleineidam L, Moreno-Grau S, Amin N, et al. New insights into the genetic etiology of Alzheimer's disease and related dementias. Nat Genet. 2022;54(4):412–36. https://doi.org/10.1038/s41588-022-01024-z.
9. Young-Pearse TL, Lee H, Hsieh Y-C, Chou V, Selkoe DJ. Moving beyond amyloid and tau to capture the biological heterogeneity of Alzheimer's disease. Trends Neurosci. 2023;46:426–44. https://doi.org/10.1016/j.tins.2023.03.005.
10. Lorenzini L, Collij LE, Tesi N, Vilor-Tejedor N, Ingala S, Blennow K, et al. Alzheimer's disease genetic pathways impact cerebrospinal fluid biomarkers and imaging endophenotypes in non-demented individuals. Alzheimers Dement. 2024. https://doi.org/10.1002/alz.14096.
11. Altmann A, Aksman LM, Oxtoby NP, Young AL, Alexander ADNI. Towards cascading genetic risk in alzheimer's disease. Brain. 2024;147:2680–90. https://doi.org/10.1093/brain/awae176.
12. Behl T, Kaur I, Sehgal A, Singh S, Albarrati A, Albratty M, et al. The road to precision medicine: eliminating the one size fits all approach in Alzheimer's disease. Biomed Pharmacother. 2022;153:113337. https://doi.org/10.1016/j.biopha.2022.113337.
13. Bartzokis G. Alzheimer's disease as homeostatic responses to age-related Myelin breakdown. Neurobiol Aging. 2011;32:1341–71. https://doi.org/10.1016/j.neurobiolaging.2009.08.007.
14. Depp C, Sun T, Sasmita AO, Spieth L, Berghoff SA, Nazarenko T, et al. Myelin dysfunction drives amyloid-β deposition in models of Alzheimer's disease. Nature. 2023;618:349–57. https://doi.org/10.1038/s41586-023-06120-6.
15. Vogel JW, Iturria-Medina Y, Strandberg OT, Smith R, Levitis E, Evans AC, et al. Spread of pathological Tau proteins through communicating neurons in human alzheimer's disease. Nat Commun. 2020;11:2612. https://doi.org/10.1038/s41467-020-15701-2.
16. Sasmita AO, Depp C, Nazarenko T, Sun T, Siems SB, Ong EC, et al. Oligodendrocytes produce amyloid-β and contribute to plaque formation alongside neurons in alzheimer's disease model mice. Nat Neurosci. 2024;27:1668–74. https://doi.org/10.1038/s41593-024-01730-3.
17. Agosta F, Pievani M, Sala S, Geroldi C, Galluzzi S, Frisoni GB, et al. White matter damage in Alzheimer disease and its relationship to gray matter atrophy. Radiology. 2011;258:853–63. https://doi.org/10.1148/radiol.10101284.
18. Maier-Hein KH, Westin C-F, Shenton ME, Weiner MW, Raj A, Thomann P, et al. Widespread white matter degeneration preceding the onset of dementia. Alzheimers Dement. 2015;11:485–e4932. https://doi.org/10.1016/j.jalz.2014.04.518.
19. Raffelt DA, Tournier J-D, Smith RE, Vaughan DN, Jackson G, Ridgway GR, et al. Investigating white matter fibre density and morphology using fixel-based analysis. Neuroimage. 2017;144:58–73. https://doi.org/10.1016/j.neuroimage.2016.09.029.
20. Dewenter A, Jacob MA, Cai M, Gesierich B, Hager P, Kopczak A, et al. Disentangling the effects of Alzheimer's and small vessel disease on white matter fibre tracts. Brain. 2023;146:678–89. https://doi.org/10.1093/brain/awac265.
21. Mito R, Raffelt D, Dhollander T, Vaughan DN, Tournier J-D, Salvado O, et al. Fibre-specific white matter reductions in Alzheimer's disease and mild cognitive impairment. Brain. 2018;141:888–902. https://doi.org/10.1093/brain/awx355.
22. Ahmadi K, Pereira JB, van Westen D, Pasternak O, Zhang F, Nilsson M, et al. Fixel-Based analysis reveals Tau-Related white matter changes in early stages of alzheimer's disease. J Neurosci. 2024;44. https://doi.org/10.1523/JNEUROSCI.0538-23.2024.
23. Luo X, Wang S, Jiaerken Y, Li K, Zeng Q, Zhang R, et al. Distinct fiber-specific white matter reductions pattern in early- and late-onset Alzheimer's disease. Aging. 2021;13:12410–30. https://doi.org/10.18632/aging.202702.
24. Solomon A, Kivipelto M, Molinuevo JL, Tom B, Ritchie CW, EPAD Consortium. European prevention of alzheimer's dementia longitudinal cohort study (EPAD LCS): study protocol. BMJ Open. 2019;8:e021017. https://doi.org/10.1136/bmjopen-2017-021017.
25. Ritchie CW, Muniz-Terrera G, Kivipelto M, Solomon A, Tom B, Molinuevo JL. The European prevention of Alzheimer's dementia (EPAD) longitudinal cohort study: baseline data release V500.0. J Prev Alzheimers Dis. 2020;7:8–13. https://doi.org/10.14283/jpad.2019.46.
26. Das S, Forer L, Schönherr S, Sidore C, Locke AE, Kwong A, et al. Next-generation genotype imputation service and methods. Nat Genet. 2016;48:1284–7. https://doi.org/10.1038/ng.3656.
27. Tesi N, van der Lee S, Hulsman M, Holstege H, Reinders MJT. SnpXplorer: a web application to explore human SNP-associations and annotate SNP-sets. Nucleic Acids Res. 2021;49:W603–12. https://doi.org/10.1093/nar/gkab410.
28. Raudvere U, Kolberg L, Kuzmin I, Arak T, Adler P, Peterson H, et al. G:Profiler: a web server for functional enrichment analysis and conversions of gene lists (2019 update). Nucleic Acids Res. 2019;47:W191–8. https://doi.org/10.1093/nar/gkz369.
29. Ashburner M, Ball CA, Blake JA, Botstein D, Butler H, Cherry JM, et al. Gene ontology: tool for the unification of biology. Nat Genet. 2000;25:25–9. https://doi.org/10.1038/75556.
30. Lin D. Others. An information-theoretic definition of similarity. Icml, vol. 98, 1998, pp. 296–304.
31. Ingala S, De Boer C, Masselink LA, Vergari I, Lorenzini L, Blennow K, et al. Application of the ATN classification scheme in a population without dementia: findings from the EPAD cohort. Alzheimers Dement. 2021. https://doi.org/10.1002/alz.12292.
32. Lorenzini L, Ingala S, Wink AM, Kuijer JPA, Wottschel V, Dijsselhof M, et al. The open-access European prevention of Alzheimer's dementia (EPAD) MRI dataset and processing workflow. NeuroImage: Clinical. 2022;35:103106. https://doi.org/10.1016/j.nicl.2022.103106.
33. Cieslak M, Cook PA, He X, Yeh F-C, Dhollander T, Adebimpe A, et al. QSIPrep: an integrative platform for preprocessing and reconstructing diffusion MRI

data. Nat Methods. 2021;18:775–8. https://doi.org/10.1038/s41592-021-01185-5.
34. Dhollander T, Connelly A. A novel iterative approach to reap the benefits of multi-tissue CSD from just single-shell (+ b = 0) diffusion MRI data. Proc Intl Soc Mag Reson Med. 2016;24:3010.
35. Dhollander T, Tabbara R, Rosnarho-Tornstrand J, Tournier JD, Raffelt D, Connelly A. Multi-tissue log-domain intensity and inhomogeneity normalisation for quantitative apparent fibre density. Proc Intl Soc Mag Reson Med. 2021;30:2472.
36. Raffelt D, Dhollander T, Tournier JD, Tabbara R, Smith RE, Pierre E, et al. Bias field correction and intensity normalisation for quantitative analysis of apparent fibre density. Proc Intl Soc Mag Reson Med. 2017;25:3541.
37. Raffelt D, Tournier J-D, Fripp J, Crozier S, Connelly A, Salvado O. Symmetric diffeomorphic registration of fibre orientation distributions. Neuroimage. 2011;56:1171–80. https://doi.org/10.1016/j.neuroimage.2011.02.014.
38. Raffelt D, Tournier J-D, Crozier S, Connelly A, Salvado O. Reorientation of fiber orientation distributions using apodized point spread functions. Magn Reson Med. 2012;67:844–55. https://doi.org/10.1002/mrm.23058.
39. Smith RE, Tournier J-D, Calamante F, Connelly A. SIFT: spherical-deconvolution informed filtering of tractograms. Neuroimage. 2013;67:298–312. https://doi.org/10.1016/j.neuroimage.2012.11.049.
40. Raffelt DA, Smith RE, Ridgway GR, Tournier J-D, Vaughan DN, Rose S, et al. Connectivity-based fixel enhancement: whole-brain statistical analysis of diffusion MRI measures in the presence of crossing fibres. Neuroimage. 2015;117:40–55. https://doi.org/10.1016/j.neuroimage.2015.05.039.
41. Wasserthal J, Neher P, Maier-Hein KH. Tractseg - fast and accurate white matter tract segmentation. Neuroimage. 2018;183:239–53. https://doi.org/10.1016/j.neuroimage.2018.07.070.
42. Fortin J-P, Parker D, Tunç B, Watanabe T, Elliott MA, Ruparel K, et al. Harmonization of multi-site diffusion tensor imaging data. Neuroimage. 2017;161:149–70. https://doi.org/10.1016/j.neuroimage.2017.08.047.
43. Lo Buono V, Palmeri R, Corallo F, Allone C, Pria D, Bramanti P, et al. Diffusion tensor imaging of white matter degeneration in early stage of Alzheimer's disease: a review. Int J Neurosci. 2020;130:243–50. https://doi.org/10.1080/00207454.2019.1667798.
44. Sudre CH, Cardoso MJ, Bouvy WH, Biessels GJ, Barnes J, Ourselin S. Bayesian model selection for pathological neuroimaging data applied to white matter lesion segmentation. IEEE Trans Med Imaging. 2015;34:2079–102. https://doi.org/10.1109/tmi.2015.2419072.
45. Smith R, Dhollander T, Connelly A. On the regression of intracranial volume in Fixel-Based Analysis. Proc Intl Soc Mag Reson Med. 2019;27:3385.
46. Dhollander T, Clemente A, Singh M, Boonstra F, Civier O, Duque JD, et al. Fixel-based analysis of diffusion MRI: methods, applications, challenges and opportunities. Neuroimage. 2021;241:118417. https://doi.org/10.1016/j.neuroimage.2021.118417.
47. Pickett EK, Henstridge CM, Allison E, Pitstick R, Pooler A, Wegmann S, et al. Spread of tau down neural circuits precedes synapse and neuronal loss in the rTgTauEC mouse model of early alzheimer's disease. Synapse. 2017. https://doi.org/10.1002/syn.21965.
48. Fowler SL, Behr TS, Turkes E, O'Brien DP, Cauhy PM, Rawlinson I, et al. Tau filaments are tethered within brain extracellular vesicles in Alzheimer's disease. Nat Neurosci. 2025;28:40–8. https://doi.org/10.1038/s41593-024-01801-5.
49. Ottoy J, Kang MS, Tan JXM, Boone L, Vos de Wael R, Park B-Y, et al. Tau follows principal axes of functional and structural brain organization in alzheimer's disease. Nat Commun. 2024;15:5031. https://doi.org/10.1038/s41467-024-49300-2.
50. Pichet Binette A, Theaud G, Rheault F, Roy M, Collins DL, Levin J, et al. Bundle-specific associations between white matter microstructure and Aβ and tau pathology in preclinical alzheimer's disease. Elife. 2021. https://doi.org/10.7554/eLife.62929.
51. Dong Y, Yu H, Li X, Bian K, Zheng Y, Dai M, et al. Hyperphosphorylated tau mediates neuronal death by inducing necroptosis and inflammation in Alzheimer's disease. J Neuroinflammation. 2022;19:205. https://doi.org/10.1186/s12974-022-02567-y.
52. Venkatramani A, Panda D. Regulation of neuronal microtubule dynamics by tau: implications for tauopathies. Int J Biol Macromol. 2019;133:473–83. https://doi.org/10.1016/j.ijbiomac.2019.04.120.
53. Alves GS, Oertel Knöchel V, Knöchel C, Carvalho AF, Pantel J, Engelhardt E, et al. Integrating retrogenesis theory to Alzheimer's disease pathology: insight from DTI-TBSS investigation of the white matter microstructural integrity. BioMed Res Int. 2015;2015:291658. https://doi.org/10.1155/2015/291658.
54. Coleman MP, Höke A. Programmed axon degeneration: from mouse to mechanism to medicine. Nat Rev Neurosci. 2020;21:183–96. https://doi.org/10.1038/s41583-020-0269-3.
55. Berghoff SA, Spieth L, Saher G. Local cholesterol metabolism orchestrates remyelination. Trends Neurosci. 2022;45:272–83. https://doi.org/10.1016/j.tins.2022.01.001.
56. Kedia S, Simons M. Oligodendrocytes in Alzheimer's disease pathophysiology. Nat Neurosci. 2025. https://doi.org/10.1038/s41593-025-01873-x.
57. Ahmed H, Wang Y, Griffiths WJ, Levey AI, Pikuleva I, Liang SH, et al. Brain cholesterol and Alzheimer's disease: challenges and opportunities in probe and drug development. Brain. 2024;147:1622–35. https://doi.org/10.1093/brain/awae028.
58. Tranfa M, Lorenzini L, Collij LE, Vállez García D, Ingala S, Pontillo G, et al. Alzheimer's disease and small vessel disease differentially affect white matter microstructure. Ann Clin Transl Neurol. 2024;11:1541–56. https://doi.org/10.1002/acn3.52071.
59. Yu M, Sporns O, Saykin AJ. The human connectome in Alzheimer disease - relationship to biomarkers and genetics. Nat Rev Neurol. 2021;17:545–63. https://doi.org/10.1038/s41582-021-00529-1.
60. Li X, Salami A, Persson J. Hub architecture of the human structural connectome: links to aging and processing speed. Neuroimage. 2023;278:120270. https://doi.org/10.1016/j.neuroimage.2023.120270.
61. Frontzkowski L, Ewers M, Brendel M, Biel D, Ossenkoppele R, Hager P, et al. Earlier Alzheimer's disease onset is associated with tau pathology in brain hub regions and facilitated tau spreading. Nat Commun. 2022;13:4899. https://doi.org/10.1038/s41467-022-32592-7.
62. Honnedevasthana Arun A, Connelly A, Smith RE, Calamante F. Characterisation of white matter asymmetries in the healthy human brain using diffusion MRI fixel-based analysis. NeuroImage. 2021;225:117505. https://doi.org/10.1016/j.neuroimage.2020.117505.
63. Vernooij MW, Smits M, Wielopolski PA, Houston GC, Krestin GP, van der Lugt A. Fiber density asymmetry of the arcuate fasciculus in relation to functional hemispheric language lateralization in both right- and left-handed healthy subjects: a combined fMRI and DTI study. Neuroimage. 2007;35:1064–76. https://doi.org/10.1016/j.neuroimage.2006.12.041.
64. Appleton J, Finn Q, Zanotti-Fregonara P, Yu M, Faridar A, Nakawah MO, et al. Brain inflammation co-localizes highly with tau in mild cognitive impairment due to early-onset Alzheimer's disease. Brain. 2025;148:119–32. https://doi.org/10.1093/brain/awae234.
65. Scott MR, Hampton OL, Buckley RF, Chhatwal JP, Hanseeuw BJ, Jacobs HI, et al. Inferior temporal tau is associated with accelerated prospective cortical thinning in clinically normal older adults. Neuroimage. 2020;220:116991. https://doi.org/10.1016/j.neuroimage.2020.116991.
66. Alves PN, Foulon C, Karolis V, Bzdok D, Margulies DS, Volle E, et al. An improved neuroanatomical model of the default-mode network reconciles previous neuroimaging and neuropathological findings. Commun Biol. 2019;2:370. https://doi.org/10.1038/s42003-019-0611-3.
67. Stern Y, Barnes CA, Grady C, Jones RN, Raz N. Brain reserve, cognitive reserve, compensation, and maintenance: operationalization, validity, and mechanisms of cognitive resilience. Neurobiol Aging. 2019;83:124–9. https://doi.org/10.1016/j.neurobiolaging.2019.03.022.
68. Lo M-T, Kauppi K, Fan C-C, Sanyal N, Reas ET, Sundar VS, et al. Identification of genetic heterogeneity of Alzheimer's disease across age. Neurobiol Aging. 2019;84:243.e1-243.e9. https://doi.org/10.1016/j.neurobiolaging.2019.02.022.
69. Bloom GS. Amyloid-β and tau: the trigger and bullet in Alzheimer disease pathogenesis. JAMA Neurol. 2014;71:505–8. https://doi.org/10.1001/jamaneurol.2013.5847.
70. Salvadó G, Ossenkoppele R, Ashton NJ, Beach TG, Serrano GE, Reiman EM, et al. Specific associations between plasma biomarkers and postmortem amyloid plaque and Tau tangle loads. EMBO Mol Med. 2023;15:e17123. https://doi.org/10.15252/emmm.202217123.
71. Horie K, Salvadó G, Barthélemy NR, Janelidze S, Li Y, He Y, et al. CSF MTBR-tau243 is a specific biomarker of tau tangle pathology in Alzheimer's disease. Nat Med. 2023;29:1954–63. https://doi.org/10.1038/s41591-023-02443-z.
72. Lantero-Rodriguez J, Montoliu-Gaya L, Benedet AL, Vrillon A, Dumurgier J, Cognat E, et al. CSF p-tau205: a biomarker of Tau pathology in alzheimer's disease. Acta Neuropathol. 2024;147:12. https://doi.org/10.1007/s00401-023-02659-w.

73. Stocker H, Möllers T, Perna L, Brenner H. The genetic risk of alzheimer's disease beyond APOE ε4: systematic review of alzheimer's genetic risk scores. Transl Psychiatry. 2018;8:166. https://doi.org/10.1038/s41398-018-0221-8.

Publisher's Note